CZECH TECHNICAL UNIVERSITY IN PRAGUE

FACULTY OF MECHANICAL ENGINEERING

DOCTORAL THESIS STATEMENT

ČESKÉ VYSOKÉ UČENÍ TECHNICKÉ V PRAZE

FAKULTA STROJNÍ

ÚSTAV PROCESNÍ A ZPRACOVATELSKÉ TECHNIKY

TEZE DISERTAČNÍ PRÁCE

Investigation of Flow and Agitation of non-Newtonian Fluids

Ing. Mehmet Ayas

Doktorský studijní program: Strojní inženýrství

Studijní obor: Konstrukční a procesní inženýrství

Školitel: *Prof. Ing. Tomas Jirout, Ph.D.*

Školitel specialista: *Doc. Ing. Jan Skocilas, Ph.D.*

Teze disertace k získání akademického titulu "doktor", ve zkratce "Ph.D."

Praha 2021

Název anglicky: Investigation of Flow and Agitation of non-Newtonian Fluids

Disertační práce byla vypracována v prezenční formě doktorského studia na Ústavu procesní a zpracovatelské techniky Fakulty strojní ČVUT v Praze.

Disertant: *Ing. Mehmet Ayas*

Ústav procesní a zpracovatelské techniky, Fakulta strojní ČVUT v Praze

Ústav procesní a zpracovatelské techniky, České vysoké učení technické v Praze, Fakulta strojní, Technická 4, 160 00 Praha 6

Školitel: *Prof. Ing. Tomas Jirout, Ph.D.*

Ústav procesní a zpracovatelské techniky, Fakulta strojní ČVUT v Praze

Ústav procesní a zpracovatelské techniky, České vysoké učení technické v Praze, Fakulta strojní, Technická 4, 160 00 Praha 6

Školitel-specialista: *Doc. Ing. Jan Skocilas, Ph.D.*

Ústav procesní a zpracovatelské techniky, Fakulta strojní ČVUT v Praze

Ústav procesní a zpracovatelské techniky, České vysoké učení technické v Praze, Fakulta strojní, Technická 4, 160 00 Praha 6

Oponenti:

Teze byly rozeslány dne: ....

Obhajoba disertace se koná dne .... v ……… hod. v zasedací místnosti č. 17 (v přízemí) Fakulty strojní ČVUT v Praze, Technická 4, Praha 6

před komisí pro obhajobu disertační práce ve studijním oboru Konstrukční a procesní inženýrství.

S disertací je možno se seznámit na oddělení vědy a výzkumu Fakulty strojní ČVUT v Praze, Technická 4, Praha 6.

Prof. Ing. Tomáš Jirout, Ph.D.

předseda oborové rady oboru Konstrukční a procesní inženýrství

Fakulta strojní ČVUT v Praze

1-Problem statement

Introduction

The present study is aimed to investigate the flow and agitation of purely viscous non-Newtonian fluids in the laminar flow regime. Firstly, rheological parameters of the investigated fluid (bovine collagen) are determined through the rectangular channel and concentric annulus for power-law and Herschel–Bulkley models.

A new method is proposed for the determination of the shear viscosity of the power-law fluids for those geometries. The provided method is then validated by experimental and numerical methods. It is found that the proposed method is successful for the determination of the shear viscosity. Then, the provided method is utilized for the prediction of friction factor of the flow of power-law fluids in non-circular channels using the Reynolds number suggested by Metzner and Reed and a simple method is suggested for the rapid calculation of the friction factor of power-law fluids in laminar regime particularly for the engineering calculations.

Finally, the power and flow characteristics of a newly designed in-line rotor-stator mixer are investigated experimentally and numerically for the Herschel–Bulkley model. The power draw of the mixer is measured experimentally and then obtained power draw values are validated by numerical simulations. The power draw and Metzner-Otto coefficients are determined from the experimentally and numerically obtained power draw results and a new slope method is suggested based on the Rieger-Novak method for mixing of viscoplastic fluids in the laminar regime. The shear and velocity profile in the mixer analyzed via numerical methods and the effect of geometrical configuration on velocity, shear, and power consumption are discussed.

Literature Survey

Basics of non-Newtonian fluids

Rheology is defined as the science of the deformation and flow of materials (Barners et al., 1989). For fluids, the applied external force is characterized by stress, and rate of deformation tensors (Darby,1976. The ratio between shear stress and the rate of deformation is a material property which is called viscosity such that

$$\tau_{ij} = 2\eta(\Delta_{ij})\Delta_{ij} \tag{1}$$

where $\eta(\Delta_{ij})$ is the material function called apparent viscosity, which is the function of the second invariant of the rate of deformation tensor (Sestak and Rieger, 2005). In the case of simple shear flow, shear rate is be described as,

$$\dot{\gamma} = \left|\sqrt{2\mathrm{II}}\right| = \sqrt{2\Delta_{ij}\Delta_{ji}} \tag{2}$$

Where $\dot{\gamma}$ is the shear rate, which is the magnitude of the rate of deformation tensor (Morrinson, 2001). The most frequently used purely viscous rheological models are given in table 1.

Pressure driven rheometers and friction factor-Reynolds number relationship for power-law fluids

The rheometer is a device that is used to determine the material function of the fluid (Morrinson, 2001; Malkin and Isayev, 2017). In pressure-driven rheometers, shear is generated by pressure gradients, and the shear rate-stress relationship is obtained from the measurement of mean velocity of the sample and corresponding pressure drop values within the fully developed region of the closed channel. The most frequently used method to imply the wall shear stress-shear rate of the power-law fluids in non-circular channels is a two-parameter model suggested by Kozicki (Kozicki et al. 1966)

$$\tau_w = K\left[\left(b + \frac{a}{n}\right)\frac{8\bar{u}}{D_h}\right]^n \tag{3}$$

is In Eq. 3, a and b are geometric parameters, these are the function of the cross-section of the channel and geometric ratios.

Table 1 Purely viscous rheological models

Power-law model	$\eta = K(\left|\sqrt{2\mathrm{II}}\right|)^{n-1}$
Cross model	$\dfrac{\eta - \mu_\infty}{\mu_o - \mu_\infty} = \dfrac{1}{1 + (\theta\left|\sqrt{2\mathrm{II}}\right|)^p}$
Carreu model	$\dfrac{\eta - \mu_\infty}{\mu_o - \mu_\infty} = (1 + (\theta\left|\sqrt{2\mathrm{II}}\right|)^2)^{(n-1)/2}$
Bingham model	$\eta = \tau_o/(\left|\sqrt{2\mathrm{II}}\right|) + \mu_p$
Herschel-Bulkley model	$\eta = \tau_o/\left|\sqrt{2\mathrm{II}}\right| + K\left(\left|\sqrt{2\mathrm{II}}\right|\right)^{n-1}$

The friction factor is one of the most frequently utilized design parameters in the industry. The friction factor is defined as the ratio of wall shear stress to the flux of inertial forces. For the fully developed, laminar flow of power-law fluids in circular duct friction factor-Reynolds number relationship is

$$\lambda \mathrm{Re}_{\mathrm{M}} = 16 \tag{4}$$

where Re_{M} is the Reynolds number suggested by Metzner and Reed (Metzner and Reed, 1955) which is given by

$$\mathrm{Re}_{\mathrm{M}} = \frac{\rho \bar{u}^{\,2-n} D^{n}}{8^{n-1} K (0.75 + 0.25/n)^{n}} \tag{5}$$

Concerning fully developed, laminar flow of power-law fluids in non-circular ducts, Kozicki (Kozicki et al. 1966) put forward the following expression for the determination of friction factor as follows

$$\lambda \mathrm{Re}_{\mathrm{G}} = 16 \tag{6}$$

Re_{G} is the generalized Reynolds number for ducts of non-circular cross-sections

$$\mathrm{Re}_{\mathrm{G}} = \frac{\rho \bar{u}^{\,2-n} {D_h}^{n}}{8^{n-1} K (b + a/n)^{n}} \tag{7}$$

Mixing of non-Newtonian fluids

Mixing is a unit operation that is carried out to reduce non-uniformities and obtaining specified property of the final products by the intensification of transport processes. For Newtonian fluids, the relationship between Po and Re is given by (Netusil and Rieger, 1992)

$$\mathrm{PoRe} = \frac{P}{\mu N^2 D^3} = C \tag{8}$$

where C is the power draw coefficient and is only depends on the geometry of the mixer. Metzner (Metzner and Otto, 1957) proposed a method for the determination of shear viscosity by introducing effective shear rate ($\dot{\gamma}_{\mathrm{eff}}$)

$$\dot{\gamma}_{\mathrm{eff}} = k_s N \tag{9}$$

In terms of yield-shear thinning fluids, Herschel–Bulkley model and Reynolds number according to Herschel–Bulkley model is given as follows

$$\mathrm{Re} = \frac{\rho N^2 D^2 k_s}{\tau_o + K (k_s N)^{n}} \tag{10}$$

Objectives of the dissertation

Mixing and transportation of the non-Newtonian fluids are commonly encountered processes in the industry. For the transportation of the non-Newtonian fluids, the essential design and process control parameter is the pressure drop which is necessary for the sizing of the channels and selection of the pumps in the system. Especially, the friction factor-Reynolds number relationship for the fully developed laminar flow of power-law fluids through non-circular channels relies on approximate methods. And in these methods, Reynolds numbers are the function of the shape of the channel and geometric ratios. Regarding the laminar mixing of the non-Newtonian fluids, the essential design and process parameter is the power consumption of the mixer, and dimensionless power and Metzner-Otto coefficients are necessary for the determination of the power demand of the mixer in the laminar regime. In the case of the mixing of viscoplastic fluids, the total energy is dissipated in the mixer to overcome yield stress for initiating flow and providing fluid flow, however, there is no explicit correlation to express them individually. Furthermore, there is no practical method for the estimation of the Metzner-Otto coefficient for the laminar mixing of viscoplastic shear-thinning fluids. Determination of the rheological parameters of the purely viscous fluids is essential for the design of the systems, prediction of the pressure drop or power demand of the mixer, and usually capillary or slit rheometers are employed for the determination of the rheological parameters. The objective of this work is listed as follows

- To show that rectangular channels and concentric annulus can be used for the determination of rheological parameters of the power-law fluids as capillary and slit rheometers. An alternative, one parameter correlation will be suggested for the estimation of the rheological parameters.

- To propose a new and very simple correlation for the prediction of the pressure drop for the laminar flow power-law fluids through non-circular channels by using geometrically independent Reynolds number and expressing friction factor-Reynolds number relationship by a simple linear equation.

- Analyzing power characteristics and flow profiles of an in-line rotor-stator mixer experimentally and numerically using shear-thinning viscoplastic fluid under the laminar regime. And then, suggesting expression to specify the effect of yield stress on the power demand of a mixer. Finally, proposing a practical method for the determination of the Metzner-Otto coefficient for the Herschel–Bulkley fluids.

3- Rectangular Channel Rheometer and a Method for the Prediction of Friction Factor of Power-Law Fluids

In this section of our study, firstly, a simple and unique method is introduced for the determination of the shear viscosity of power-law fluids utilizing rectangular channels and capillary annulus. The suggested method is compared with existing methods analytically, experimentally, and employing numerical simulations. Then, based on the suggested method, a very simple equation is introduced for the prediction of the friction factor of the power-law fluids in non-circular channels.

1- Rectangular and capillary annulus rheometers

The shear viscosity is one of the most measured rheological properties of the fluids and t measurement of shear viscosity is carried out by using a slit or capillary rheometers at high shear rates of the fluid. In this section, a simplified method is proposed for the measurement of shear viscosity using only one parameter especially for the rectangular and capillary annulus cross-sections. The correlation is given in Eq. 6 quite successful to characterize shear stress- shear rate relationship but the method requires two geometrical parameters. A simpler approach can be obtained by expressing the wall shear stress -wall shear rate relationship by one parameter C instead of a and b relying on the method suggested by Ayas (Ayas et al. 2019-a). If the term $(\mathrm{b}+\mathrm{a}/\mathrm{n})^{\mathrm{n}}$ in Eq. 3 is defined as α.

$$\alpha = (\mathrm{b}+\mathrm{a}/\mathrm{n})^{\mathrm{n}} \tag{11}$$

The ratio of α to $(0.75+0.25/\mathrm{n})^{\mathrm{n}}$ is ε

$$\varepsilon = \left(\frac{4(\mathrm{bn}+\mathrm{a})}{3\mathrm{n}+1}\right)^{\mathrm{n}} \tag{12}$$

The curves of the ε versus flow index (n) for rectangular channel and concentric annulus with the aspect ratios between zero and one are demonstrated in figure 1. Ayas et al. (Ayas et al., 2019-a; Ayas et al., 2020-a) has suggested that the ε can be assumed as a linear function of flow index for $0 < \mathrm{n} < 1$ for the rectangular channel and concentric annulus. Hence Eq. 12 can be expressed as follows

$$\varepsilon = \mathrm{Mn}+\mathrm{N} \tag{13}$$

As flow index n approaches zero, the limit of ε in Eq. 12 equals one which can be seen from the plot in figure 1.

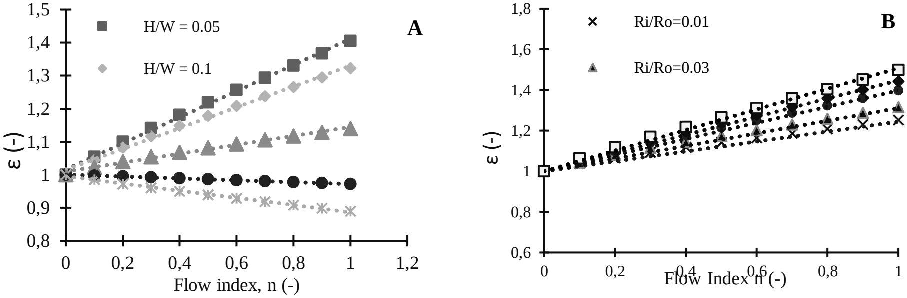

Figure 1 Relation between ratio ε and flow index n, (A) – Rectangular channel (B)-Concentric Annuli (Ayas et al., 2019-a; Ayas et al., 2020-a)

$$\lim_{n\to 0}\left(\frac{4(bn+a)}{3n+1}\right)^n = \lim_{n\to 0}(Mn+N) = 1 \tag{14}$$

From the obtained correlations given in Eq. 12 and Eq. 13, the Eq. 11 (α) can be expressed by one parameter as follows

$$\alpha = (b + a/n)^n = (Mn+1)\left(\frac{3n+1}{4n}\right)^n \tag{15}$$

Consequently, Eq. 3 can be stated as

$$\tau_w = K\left(\left(\frac{C}{16}-1\right)n+1\right)\left[\left(\frac{3n+1}{4n}\right)\frac{8u}{D_h}\right]^n \tag{16}$$

and the wall shear rate is

$$\dot{\gamma}_w = \left[\left(\frac{C}{16}-1\right)n+1\right]^{1/n}\left(\frac{3n+1}{4n}\right)\frac{8u}{D_h} \tag{17}$$

As seen from Eq. 16 and Eq. 17, the wall shear rate-wall shear stress can be expressed only one geometrical coefficient C instead of a and b (Ayas et al., 2019-a; Ayas et al., 2020-a). A similar correlation can be obtained by using the parameters of parallel plates ($a = 0.5$ and $b = 1$). If the ratio of $(1 + 0.5/n)^n$ to Eq. 28 is defined as ε'

$$\varepsilon' = \frac{(1+\frac{0.5}{n})^n}{(b+\frac{a}{n})^n} = \left[\frac{2n+1}{2(bn+a)}\right]^n \tag{18}$$

The variation of ε' with respect to flow index in the range of $0 < n < 1$ and geometric ratios for the investigated cross-sections are given in figure 2. From the regression analysis ε' can be assumed as a linear function of flow index and geometric ratios.

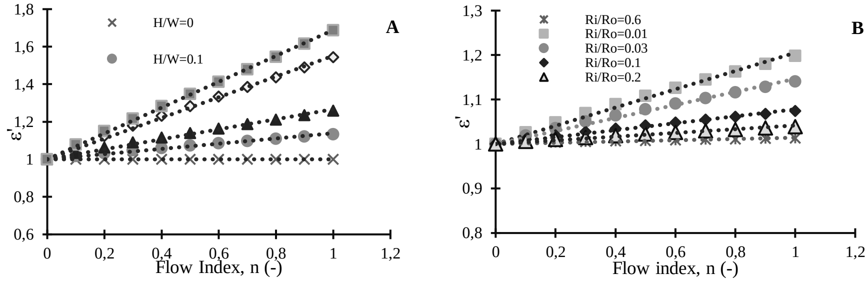

Figure 2 Approximated linear variation of ε' (A)- Rectangular channel, (B) - concentric annulus

Therefore Eq. 18 can be written for $0 < n < 1$ as

$$\varepsilon' = M'n + N' \tag{19}$$

As flow index n approaches zero, the limit of ε' equals one, hence the constant N'should be equal to one, and the term $(b + a/n)^n$ can be written as

$$\alpha = (b + \frac{a}{n})^n = \frac{\left(1 + \frac{0.5}{n}\right)^n}{M'n + 1} \tag{20}$$

The value of M' can be determined from the Newtonian flow case as

$$M' = \frac{24}{C} - 1 \tag{21}$$

and substituting Eq. 20 into Eq. 3, wall shear stress is given as follows

$$\tau_w = \frac{K}{M'n + 1}\left[\left(\frac{2n + 1}{2n}\right)\frac{8u}{D_h}\right]^n \tag{22}$$

Validation and discussion

The provided method is validated analytically and experimentally. Ayas et al. (Ayas et al., 2019-a, Ayas et al., 2020-a) validated the suggested α functions given in Eq. 15 and Eq. 20 with Eq. 11 analytically. From the comparison, the maximum deviation between the equations was found less than 2.5%. The proposed correlation has been verified through experimental data available in the literature (Skocilas et al, 2017). Experiments were conducted in a piston-driven extrusion rheometer for the investigation of the rheological properties of the water solution of bovine collagen with a mass fraction of 9.5 % and density of 1100 kg/m^3. The channel used in the experiment has a rectangular cross-sectional geometry with a length of 200 mm and a width of 20 mm (see figure 3). Two different heights of channels were utilized in the experiment with the heights of 2 mm, and 4 mm. From the experimental data, obtained overall flow curve for the dies with H of 2 mm and 4 mm with a coefficient of determination of 0.98. The flow index has been found as 0.3 and consistency is 1060 $\mathrm{Pa.s^n}$.

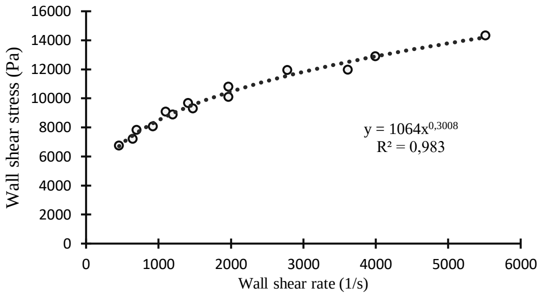

Figure 3 Overall flow curve for H = 2 mm and H = 4 mm

A method for predicting the friction factor of power-law fluids in non-circular channels

In this section, an alternative, simple method is proposed for the prediction of friction factor for the flow of power-law fluids in non-circular channels under the laminar flow regime. The simplification is achieved by using the Reynolds number suggested by Metzner and Reed and then a very simple correlation is introduced to express the relationship between friction factor and Reynolds number ($\mathrm{Re_M}$) based on the assumption given in Eq. 5 in the previous section (Ayas et al., 2020-a) for non-circular cross-sectional shapes (i.e. elliptical, concentric annuli, symmetrical L-shape, isosceles triangle, eccentric annuli, square duct with a central cylindrical core).

The proposed simplified method is based on analyzing the relationship between the Reynolds number suggested by Metzner and Reed ($\mathrm{Re_M}$) and by Kozicki ($\mathrm{Re_G}$) for shear-thinning fluids (Ayas et al., 2019-a). The Reynolds number defined by Metzner and Reed ($\mathrm{Re_M}$) for a rectangular channel can be written as

$$\mathrm{Re_M} = \frac{\rho u^{2-n} {D_h}^n}{8^{n-1} K \left(\frac{3n+1}{4n}\right)^n} \tag{22}$$

The ratio of $\mathrm{Re_M}$ to $\mathrm{Re_G}$ is

$$\frac{\mathrm{Re_M}}{\mathrm{Re_G}} = \left(\frac{4(bn+a)}{3n+1}\right)^n \tag{24}$$

As seen, the ratio $\mathrm{Re_M}/\mathrm{Re_G}$ is equal to the defined function ε. Using the linear approximation for ε given in Eq. 13 for the flow indexes in the range of $0 < n < 1$, the ratio $\mathrm{Re_M}/\mathrm{Re_G}$ is equal to

$$\frac{Re_M}{Re_G} = Mn + N \tag{25}$$

It has been shown that the value of coefficient N is equal to. Substituting Eq. 25 into Eq. 6, the final expression is given as follows

$$fRe_M = (C - 16)n + 16 \tag{26}$$

It can be seen that for the circular channel ($C = 16$) Eq. 26 reduces to Eq. 4. It has been pointed out by Ayas et al. (Ayas et al. 2020-a) that obtained linear approximation of ε exists for cross-sectional shapes of elliptical, concentric annuli, symmetrical L-shape, eccentric annuli, square duct with a central cylindrical core (Ayas et al.,2020-a) which is shown in figure 5.

Alternatively, a different correlation can be obtained in terms of the parameters of parallel plates ($a = 0.5, b = 1$) especially for the channels with a narrow gap. It has been found that ε' indicates better linearity for the channels with narrow gaps. The alternative correlation for the friction factor Reynolds relationship is

$$fRe'_M = \frac{16C}{(24 - C)n + C} \tag{27}$$

where Re'_M is

$$Re'_M = \frac{\rho \bar{u}^{\,2-n} {D_h}^n}{8^{n-1} K \left(1 + \frac{1}{2n}\right)^n} \tag{28}$$

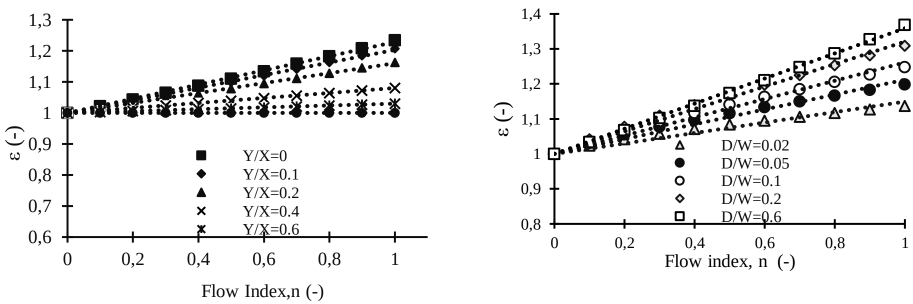

Elliptical

Square duct with a central cylindrical core

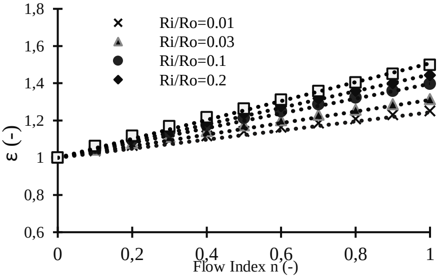

Concentric annuli

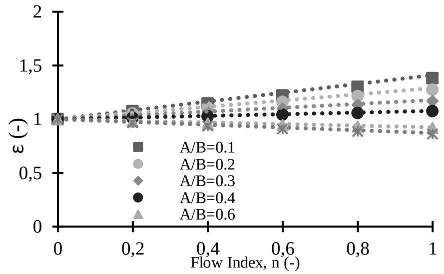

L-shape

Figure 4 The linear relation of ε and flow index (Ayas et al., 2020-a)

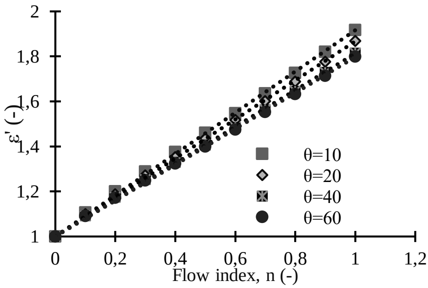

Isosceles triangle

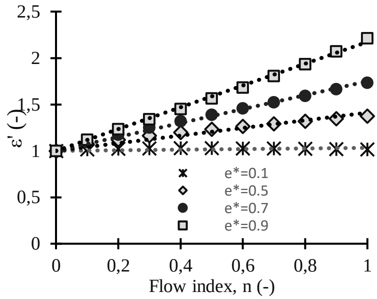

Eccentric annuli for $\kappa = 0.9$

Figure 5 The linear relation of ε' and flow index

The critical value of Reynolds number (Re_M) for the onset of the turbulent region has been considered as 2100 and the effect of the shape of cross-section on critical Reynolds number is neglected in this study.

Validation and discussion

The suggested method for the prediction of friction factor is initially compared with the method suggested by Kozicki by comparing relative deviation. The relative deviation is defined as

$$\text{Deviation } = \frac{(\lambda_G - \lambda_M)}{\lambda_G} * 100 \tag{29}$$

In Eq. 29, λ_G indicates the friction factor obtained from Kozicki's method and λ_M represents the friction factors for one-parameter models from Eq. 26.

The results of comparisons for the eccentric channel of $\kappa = 0.9$, square duct with a centered cylindrical core, and symmetrical L-shape are depicted in figure 6. As seen in figure 6, the deviations between Kozicki's method (λ_G) and proposed method in Eq. 26 (λ_M) increase with the increasing values of e* and maximum deviation has been found less than 4 % for e*=0.9. Regarding the square duct with a centered cylindrical core and symmetrical L-shape suggested method in Eq. 26 maximum deviation has been found less than 2%. Another experimental verification (Ayas et al., 2019-a) was carried out using experimental data obtained by Hartnett (Hartnett and Kostic, 1985). Results of experimental data and calculated friction factor values according to Eq. 6 and Eq. 26 are shown in table 2. The maximum deviation has been found less than 9 % and calculated friction factor values from Eq. 6 and Eq. 26 are very close.

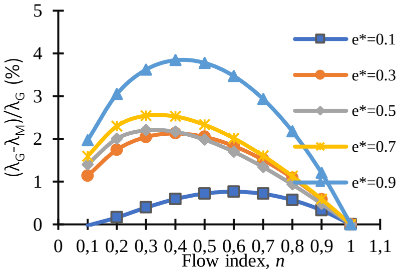

Eccentric channel of $\kappa = 0.9$

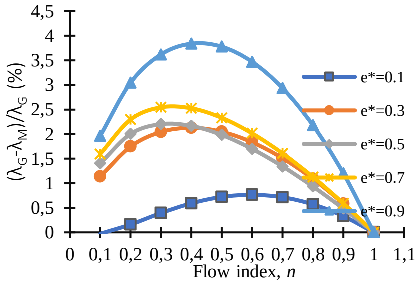

The square duct with a centered cylindrical core

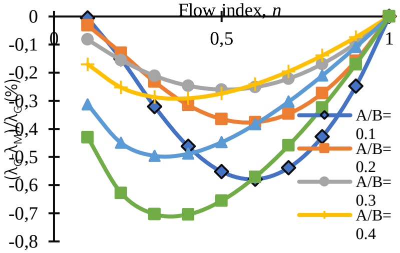

Symmetrical L-shape

Figure 6 Relative deviations of λ_M and λ_G with respect to Kozicki's method

Table 2 Result of validation Eq. 26 and experimental data (Hartnett and Kostic,1985)

n	Re_M	Re_G	λ_{exp}	λ (Eq. 6)	λ (Eq. 26)
0.542	297	292.5	0.04951	0.0539	0.0538
0.563	616	606.3	0.02414	0.0260	0.0260
0.577	749	736.9	0.02177	0.0214	0.0214
0.59	1291	1269.7	0.01161	0.0124	0.0124
0.601	1715	1686.2	0.00875	0.0093	0.0093
0.616	2170	2132.6	0.00735	0.0074	0.0074

The other comparison has been carried out by performing numerical methods using ANSYS FLUENT 15 for, isosceles triangles, eccentric and concentric annulus, elliptical, symmetric L-shape, and a square duct with central cylindrical core cross-sections (Ayas et al., 2019-a; Ayas et al., 2020-a). Simulations were carried out for isosceles triangle of 90° and eccentric channel of κ=0.7, e ∗=0.9 for the flow indexes (n) of 0.4, 0.5, 0.6, 0.7, 0.8 and concentric annulus, elliptical, symmetric L-shape and a square duct with central cylindrical core cross-sections for $n = 0.5$ and various aspect ratios. The consistency (K) was chosen as 0.5 $Pa.s^n$ and the mean velocity was taken as 1.5 m/s for all simulations. For the boundary conditions, the inlet was chosen as velocity inlet, the outlet was selected as pressure outlet and the walls were taken stationary wall. For the solution method, the simple scheme was specified for pressure-velocity coupling and second-order pressure and momentum were selected for spatial discretization. The convergence criteria was taken for the continuity residual below 10^{-6}.

Numerically evaluated λRe_M values were compared with suggested methods and as well as conventionally used methods (Kozicki's and Delplace's methods). The results of the comparison are illustrated in figure 7. For concentric annulus, Eq. 26 yields better results than Kozicki et al. and Delplace and Leuliet's methods, and maximum deviation remain less than 5% for those three methods. For elliptical and L-shape channels predicted λRe_Mvalues by Kozicki et al.'s method and Eq. 26 are very close and Deplace and Leuliet's method yields less accurate results than the other two methods. For those two geometries, Eq. 26 ensures to predict friction factor less than 4% deviation. For Square duct with a centered cylindrical core, Koziki's method gives better results than Eq. 26 and Delplace's method especially for the higher values of D/W. The difference between determined λRe_M values have been examined for $D/W = 0.8$ and different values of flow indexes.

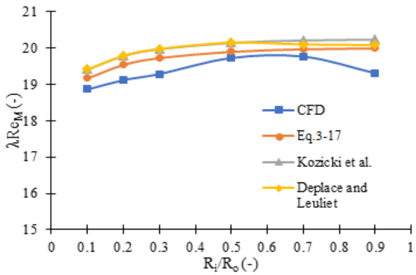

a- Concentric annulus, n=0.5 (-)

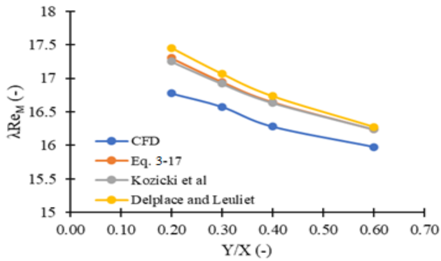

b- Elliptical channel, n=0.5 (-)

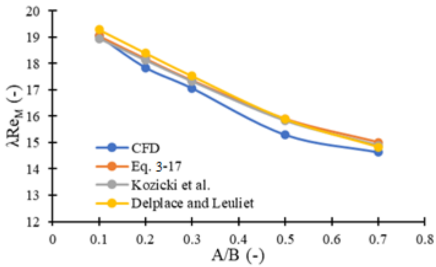

c- Symmetrical L-shape, n=0.5 (-)

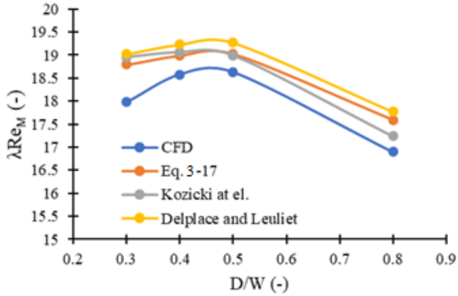

d- Square duct with a centered cylindrical core, n=0.5 (-)

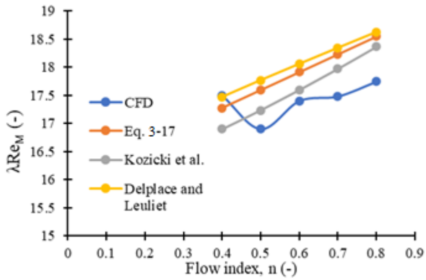

e- Square duct with a centered cylindrical core, D/W=0.8

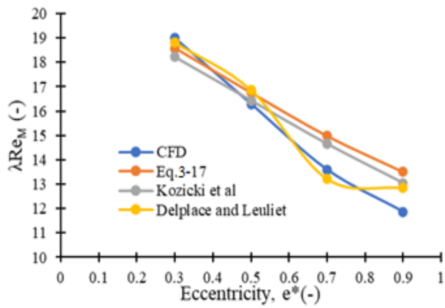

f- Eccentric channel κ=0.7

Figure 7 The comparison between approximate models and results of simulations

It was found that Eq. 26 gives better results than Delplace's method and the maximum deviation remains less than 5 % for the three methods. The difference between evaluated $\lambda \mathrm{Re_M}$ is checked for the eccentric channel of $\kappa = 0.7$ and $0.3 \leq e* \leq 0.9$. It was found that investigated three methods provide a successful result for $0.3 \leq e* \leq 0.5$, with a deviation of less than 4 % but for e*> 0.5, deviation increases as eccentricity increases for the three methods. Especially Eq. 26 yields unsatisfactory results with a deviation of 15 % for e*=0.9.

Conclusion

In this section, rectangular channels of aspect ratios greater than 0.1 and concentric annulus were investigated for the measurement of shear viscosity of power-law fluids which is the most frequently used rheological model in the industry. An approximate one-parameter model was suggested for the determination of the wall shear rate for the power-law model. The provided correlation was validated using experimental data and compared with conventionally used methods. From the comparisons, it was deduced that provided correlation enables to determine shear viscosity of power-law fluids.

The suggested correlation for the prediction of friction factor can be used successfully for the cross-sectional geometries of the rectangular, concentric annulus, symmetrical L-shape, square duct with a central cylindrical core, eccentric annulus with low aspect ratios, elliptical cross-sectional geometries for $0 < n < 1$ with a deviation of less than 5% and the model ensures slightly better results than other one parameter Delplace and Leuliet's method for those geometries. The alternative correlation based on Reynolds number $\mathrm{Re'_M}$ specified in Eq. 44 is giving better results for the prediction of friction factor for the geometries with narrow clearances and isosceles triangles, hence it is recommended to use infinite plate parameters for the channels with narrow gaps.

4 -Agitation of viscoplastic fluid in in-line rotor-stator mixer

Mixing is one of the most frequently used unit operations in the industry which is carried out to reduce gradients of specified properties such as concentration, temperature, etc. Agitation of viscoplastic fluids gives rise to the formation of the well-mixed region in the vicinity of the impeller, and dead zones are generated next to the wall of the mixing vessel and which leads to poor mixing. In such cases, a more efficient mixing operation can be achieved by agitation viscoplastic fluids in rotor-stator mixers.

The design of the studied mixer was created by the research and development team of the Process engineering department by Dr. Jan Skocilas, Ing. Dr. Jiri Moravec Ing., Dr. Lukas Kratky, and Prof. Dr. Tomas Jirout Ing. The newly designed in-line rotor-stator mixer consists of two serial mixing heads which are installed in a cylindrical barrel and two impellers were mounted on the same shaft. For the designed mixer, the radial clearance (c_r) between the rotor and stator is 3 mm constant. The axial clearances (c_a) between rotor and stator can be adjusted according to requirements of the process. The agitation of the mixer is provided by 45^o four-pitch blade impellers with a diameter (D) of 194 mm and the diameter of the stator (Z) is 200 mm. The inlet and outlet of the mixer are hollow disks and the shaft of the mixer is located at the center of the disk. (Ayas et al., 2019-c).

In this section energy consumption, flow profile of given in-line rotor-stator mixers are investigated experimentally and numerically. Power consumption of the rotor-stator mixer is measured using yield shear-thinning fluid experimentally and obtained power consumption values are validated using numerical methods by ANSYS FLUENT. Then, power consumption, flow field, velocity profile, and shear profile will be studied using numerical methods for Newtonian, power-law, and Herschel–Bulkley model. Mixing Reynolds number-power number relationship are discussed.

Theory

In terms of in-line rotor-stator mixers, the generated power is the sum of power created by impellers (P_R) and power of flowing fluid (P_f) between the inlet and outlet sections of the mixer (Kowalski, 2009).

$$P_{total} = P_R + P_f \tag{30}$$

The total power number (Cooke et al., 2012) for an in-line rotor-stator mixer alternatively can be written as follows

$$Po = Po_R + kN_Q \tag{31}$$

Where k is power flow constant and N_Q is the flow number. It was suggested that the effect of fluid flow on the power consumption (P_f) of a rotor-stator mixer in a laminar flow regime is neglected (Cooke et al., 2012). Introducing effective shear rate, Hedstrom number for Herschel–Bulkley can be stated as

$$He = \frac{\rho\tau_0 D^2}{(K(k_s N)^{n-1})^2} \tag{32}$$

and using Reynolds number (Re_{MO}) suggested by Metzner and Otto, Bingham number is described as

$$Bi = \frac{He}{Re_{MO}} = \frac{\tau_0}{K(k_s)^{n-1}(N)^n} \tag{33}$$

Using Bi and Re_{MO}, Eq. 27 can be stated alternatively as follows.

$$PoRe_{MO} = \frac{C}{k_s} Bi + C \tag{34}$$

Dividing both sides of Eq. 52 by $(k_s)^{n-1}$, the Eq. 52 is expressed by Re_{RN} such that

$$\mathrm{PoRe_{RN}} = \frac{\mathrm{C}}{\mathrm{k_s}}\mathrm{Bi}^* + \mathrm{C}(\mathrm{k_s})^{\mathrm{n}-1} \tag{35}$$

where Bi* is (Archard et al., 2006)

$$\mathrm{Bi}^* = \frac{\tau_0}{\mathrm{K}(\mathrm{N})^{\mathrm{n}}} \tag{36}$$

According to Eq. 35, the plot of $\mathrm{PoRe_{RN}}$ versus Bi^* for the same fluid at different velocities should be linear and the slope of that curve is equal to $\mathrm{C}/\mathrm{k_s}$. Hence, $\mathrm{k_s}$ the value of the mixer can be calculated from the slope of the linear curve if the C value is known. On the other hand, power number according to Eq. 35 can be expressed as follows (Ayas et al., 2020-b)

$$\mathrm{Po_R} = \mathrm{Po_Y} + \mathrm{Po_S} \tag{37}$$

where $\mathrm{Po_Y}$ indicates the power number for overcome yield stress and $\mathrm{Po_S}$ represents the power number of the sheared flow and can be defined by the following equation.

$$\mathrm{Po_Y} = \frac{\mathrm{CBi}^*}{\mathrm{Re_{RN}k_s}} \tag{38}$$

$$\mathrm{Po_S} = \frac{\mathrm{C}(\mathrm{k_s})^{\mathrm{n}-1}}{\mathrm{Re_{RN}}} \tag{39}$$

For an efficient mixing process of yield-shear thinning fluid, $\mathrm{Po_S}$ should be high enough since mixing efficiency is proportional to the created shear in the mixer in the laminar flow regime (Ayas et al., 2020-b). Hence, mixing process efficiency in the laminar regime can be defined as

$$\mathrm{X} = \frac{\mathrm{Po_S}}{\mathrm{Po_Y} + \mathrm{Po_S}} = \frac{\mathrm{Po_S}}{\mathrm{Po}} \tag{40}$$

From Eq. 40, it is obvious that the efficiency increases with rotor speed and Metzner-Otto coefficient and decreases by yield stress.

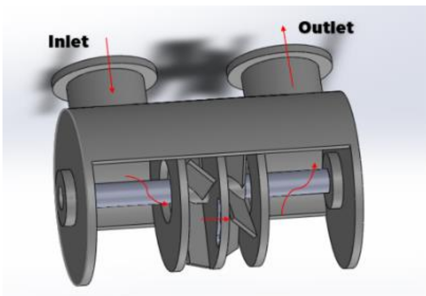

Figure 8 Investigated rotor-stator mixer

Experiment and simulation

The investigated in-line rotor-stator mixer has been designed with the aim of preparation of homogeneous dispersion of dye in collagen matter which is an extremely viscous material. The pressure drop of the fluid between the inlet and outlet sections and temperature increase due to viscous heat dissipation and the power consumption of the investigated mixer was measured. All measurements were taken for the axial clearances of 1 mm, 2 mm, and 3 mm and rotor speeds of 150 RPM, 300 RPM, and 500 RPM. The water solution of the bovine collagen with a mass fraction of 7.7 % was used as a test material. The rheological properties of the test fluid were examined by a capillary rheometer. It was found that the fluid exhibits a yield shear-thinning characteristic and obtained rheological properties are $\tau_0 = 4600$ Pa, K=420 Pa.s^n, n=0.34 (Skočilas et al., 2016). Iced water was used as a coolant. The pressure of fluid was measured by a diaphragm manometer which is located at the inlet of the barrel and at the outlet of the barrel the pressure of the fluid was considered as zero-gauge pressure. The optimum flow rate of the collagen was determined as 6 kg/min.

Three-dimensional numerical simulations (Ayas et al., 2020-b) were carried out in order to verify experimental data, for the determination of the power draw coefficient C and analyzing velocity and shear profile within the mixing heads. After creating the fluid domain, the next step is the generation of grids (meshes) in the ANSYS workbench. The geometry of the heads is not uniform, thus unstructured meshes were created. The simulation of investigated in-line rotor-stator mixer is carried out for the steady-state flow case, under the laminar flow regime and isothermal flow case, and MRF method was applied to model rotation of the impellers. Regarding boundary conditions, the inlet of the barrel is assigned as a mass flow inlet, and the outlet of the barrel is pressure outlet.

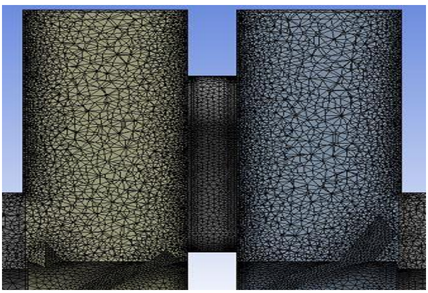

Figure 9 Created grids for the simulations

Shaft and impellers are selected as moving wall. It has been assumed that the effect of wall-slip is negligible. The SIMPLE scheme was applied for the pressure-velocity coupling and, second-order pressure and second-order upwind velocity schemes were utilized. Convergence criteria for the continuity is below the 10^{-9} for the Herschel–Bulkley model, 10^{-6} for the power-law model, and Newtonian case.

Result and Discussions

The results of measured power consumption values are given in figure 10. As seen from the figure, the power consumption of the mixer varies almost linearly with the rotational speed of the rotor due to the effect of the high yield stress value of the fluid and c_a does not have a significant effect on the power draw.

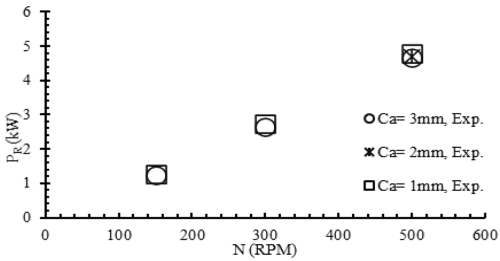

Figure 10 Experimentally measured power values

The power arising from fluid flow (P_f) is much less than the power of the rotor, so the power of fluid flow on the power consumption of the mixer is negligible. From the experimentally measured power consumption values, determined Po and Reynolds number (Re_{RN}) values are given in table 3.

Table 3 Experimentally determined Po and Re values

c_a mm	Impeller Speed RPM	Po (-)	Re_{RN} (-)
3	150	266.4	0.451
3	300	70.7	1.425
3	500	26.67	3.33
2	500	26.61	3.33
1	150	266.8	0.451
1	300	71.46	1.425
1	500	27.33	3.33

As seen from table 3, the power number decreases with increasing values of the rotor speed and Reynolds numbers, which confirms that the experiments were carried out in the laminar flow regime. The results of numerically evaluated power consumption values of the investigated mixer and a comparison with experimental data are depicted in figure 11. The difference between numerically and experimentally obtained values is less than 5% which is in an acceptable range.

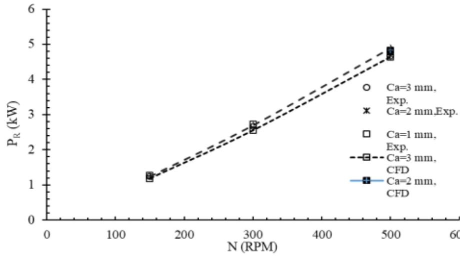

Figure 11 Experimentally and numerically obtained power draw values

The power constant C values have been determined for c_a of 1 mm, 2 mm, and 3 mm by simulations for the Newtonian case in the laminar regime. From the result of simulations, the acquired Po versus the Re curves and evaluated C values are given in figure 13. The values of the Metzner-Otto coefficient k_s for the investigated in-line mixer have been evaluated from the experimentally and numerically obtained methods given in table 4.

Table 4 Experimentally and numerically determined k_s values (Ayas et al., 2020-b)

N	c_a=1 mm		c_a=2 mm		c_a=3 mm	
RPM	k_s (Exp.)	k_s (CFD)	k_s (Exp.)	k_s (CFD)	k_s (Exp.)	k_s (CFD)
150	82.5	84.0	*	*	57.5	61.6
300	84.4	84.5	*	*	59.2	62.5
500	86.2	83.7	72.5	70.2	60.8	61.3
Average	84.4	84.1	72.5	70.2	59.2	61.8

From the experimentally and numerically obtained power consumption values, created $PoRe_{RN}$ versus Bi* curves are illustrated in figure 12. From the curves of CFD results, k_s values are found as 84.4 and 61.8 for axial clearances (c_a) of 1 mm and 3 mm respectively which are identical to obtained results of the direct method given in table 4. On the other hand, from the experimental obtained k_s values were found as 73 and 53.4 for the

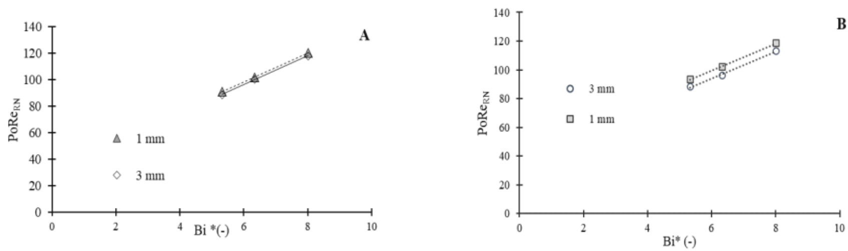

Figure 12 P_oRe_{RN} versus Bi* curves (A)-Experiment, (B)- CFD

axial clearances of 1 mm and 3 mm which shows a reasonable agreement, namely there is a 9 % deviation for $c_a = 3$ mm and 13 % deviation for $c_a = 1$ mm and the reason deviation may arise from the measurement errors, however, results are still in the acceptable range. Another studied parameter associated with the power draw of the mixer is the efficiency (X) given in Eq. 40. The evaluated Po_y, Po_S and X values from the results experimental and numerical data are given in table 5.

Table 5 Po_y, Po_S and efficiency values

c_a (mm)	N (RPM)	P_o (Exp.)	Po_y (Exp.)	Po_S (Exp.)	X (Exp.)	Po (CFD)	Po_y (CFD)	Po_S (CFD)	X (CFD)
3	150	266	178.3	88.2	0.33	250.8	166.5	84.3	0.34
3	300	70.4	43.3	27.4	0.39	67.5	41.1	26.4	0.39
3	500	26.7	15.2	11.5	0.43	26.5	15.1	11.5	0.43
2	500	26.9	14.9	12.0	0.45	27.6	14.9	12.0	0.43
1	150	266.78	171.1	95.6	0.36	262.6	168.1	94.5	0.36
1	300	71.5	41.7	30.5	0.41	71.6	41.8	29.8	0.42
1	500	27.3	14.7	12.5	0.46	28.0	15.2	12.8	0.46

the c_a values of 1 mm, 2 mm, and 3 mm. The shear rate distribution is investigated in midplanes between rotor and stator only. From the result of simulations, evaluated non-dimensional shear rate ($\gamma^* = \dot{\gamma}/N$) curves for the c_a values of 1 mm and 3 mm are given in figure 13. From the figures, it can be concluded that the evaluated dimensionless shear profile is independent of rotor speed and significantly hinge upon the geometry.

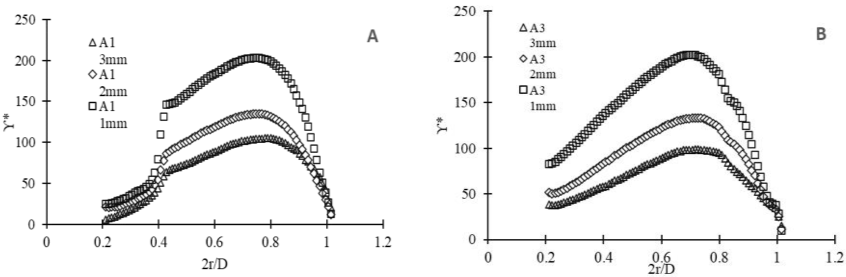

Figure 13 Effect of axial clearance on the dimensionless shear rate for N=500 RPM

Conclusion

In this chapter, the power characteristics of a newly designed in-line rotor-stator mixer have been investigated experimentally and numerically. The experiments were carried out for the three rotational speeds of the rotor and three axial clearances between rotor and stator using viscoplastic shear-thinning fluid. The power demand of the mixer and the pressure gradient between inlet and outlet sections of the mixer were measured by experiments. It was shown that experimentally and numerically acquired power consumption values were in good agreement with a 6 % maximum deviation. It was shown that evaluated Metzner-Otto coefficients from the experimental and numerical data are very close. A new correlation was proposed to express the power characteristics of a mixer for the Herschel–Bulkley model.

According to the suggested correlation, the total power consumption of a mixer can be written as the sum of the power necessary to overcome yield stress, and the required power shear flow and corresponding power numbers (Po_y, Po_s) were defined. By using defined Po_y and Po_s the new term efficiency (X) was introduced to analyze the shear efficiency of the agitation of yield stress fluids. It was shown that higher shear rates can be acquired by reducing axial clearance and the power draw of the mixer is significantly varies with the rotor speed.

5-Annotation

This work deals with the measurement of rheological properties of the purely viscous non-Newtonian fluid, prediction of friction factor, and power and flow characteristics of an in-line rotor-stator mixer. Firstly, a method is suggested for the evaluation of the rheological parameters for the power-law fluids using the rectangular channel and concentric annuli. According to the method, the relationship between wall shear rate and wall shear stress can be represented by one geometrical parameter for any aspect ratios. It has been shown that rectangular channels and concentric annulus can be used for the determination of rheological parameters the same as slit and capillary rheometers for the power-law fluids. The provided method is validated by comparing the most frequently used methods and through numerical simulations and it was found that the suggested method can predict friction factor accurately.

Finally, the power characteristics and flow field of a newly designed in-line rotor-stator mixer have been analyzed experimentally and numerically according to the determined rheological parameters in the previous section. Initially, the power draw of the mixer has been measured experimentally for the three rotational speeds of the impeller and three different axial clearances of the mixer, and then obtained power draw results have been validated by numerical simulation, and a good agreement was found between the numerically and experimentally obtained power values. The Newtonian power draw coefficient has been calculated by numerical simulations and then, Metzner-Otto constants have been determined from the experimentally and numerically obtained power draw results. It was found that determined Metzner-Otto coefficients from the experimental and numerical methods are in good agreement. A slope method was proposed for the determination of the Metzner-Otto coefficient for the Herschel–Bulkley model and it was shown that the introduced method is successful for the prediction of the Metzner-Otto coefficient. In the final step, the effect of axial clearance on velocity and shear profile is discussed and it was found that axial clearance has a remarkable effect on flow profile on the agitated fluid in the mixer.

Nomenclature

a, b	Geometrical parameters of Eq. 3 (-)
A, B	Dimensions of the symmetrical L-shape duct (m)
Bi^*	Bingham number for Herschel-Bulkley model (-)
C	Geometric parameter of the Newtonian fluids (-)
C	Newtonian power constant (-)
d, D	Diameter (m)
D_h	Hydraulic diameter (m)
e^*	Dimensionless eccentricity (-)
e	Length of eccentricity (m)
h	Height of impeller blade (m)
H	Height of the rectangular duct (m)
He	Hedstrom number (-)
K	Fluid consistency ($Pa.s^n$)
k_s	Metzner-Otto coefficient (-)
L	Length (m)
m	Consistency for Casson model ($Pa.s^n$)
M	Number of mesh elements (-)
M, N	Parameters of Eq. 13 (-)
M', N'	Parameters of Eq. 19 (-)
n	Flow behavior index (-)
N	Rotational velocity (RPM)
p	Pressure (Pa)
p	Parameter of Cross model (-)
P	Power (W)
Po	Power number (-)
R	Radius (m)
Re	Reynolds number for Newtonian fluids (-)
Re_G	Generalized Reynolds number by Kozicki (-)
Re_M	Reynolds number, as defined by Metzner and Reed (-)
Re_M'	Reynolds number, as defined in Eq 3-19 (-)
Re_{MO}	Reynolds number defined by Metzner and Otto (-)
Re_{RN}	Reynolds number defined by Rieger and Novak (-)
t	Time (s)
T	Torque (N.m)
u	Velocity (m/s)
$\bar{u}$	Mean velocity (m/s)
V	Volume (m^3)
$\dot{V}$	Volume flow rate (m^3/s)
W	Width of the rectangular duct (m)
X, Y	Major and minor axes of an elliptical duct (m)

Greek letters

α	Function given in Eq. 11
ε	Ratio of Re_M to Re_G (-)
ε'	Ratio in Eq. 18 (-)
θ	Apex angle of an isoscale triangle (°)

θ	Parameter of Carreu model
σ	Total stress (Pa)
λ	Fanning friction factor (-)
$\dot{\gamma}$	Shear rate (s^{-1})
$\dot{\gamma}_N$	Newtonian wall shear rate (s^{-1})
$\dot{\gamma}_w$	Wall shear rate (s^{-1})
η	Apparent viscosity (Pa.s)
μ_0	Zero shear viscosity (Pa.s)
μ_∞	Infinite shear viscosity (Pa.s)
μ_a	Apparent viscosity (Pa.s)
μ_p	Plastic viscosity (Pa.s)
ρ	Density ($kg.m^{-3}$)
τ	Shear stress (Pa)
τ_o	Yield Stress (Pa)
τ_w	Wall shear stress (Pa)
Δ	Rate of deformation tensor (1/s)

References

1. Archard A. D., Marouche M., Boisson H.C., Hydrodynamics and Metzner–Otto correlation in stirred vessels for yield stress fluids, Chem. Eng. Sci., **125**, 15-24, (2006).
2. Barners H.A, Hutton J.F, and Walters K., An introduction to rheology 1st edition, Netherland, Elsevier, (1989)
3. Bertrand F., Tanguy P. A., Fuente E. B., A new perspective for the mixing of yield stress fluids with anchor impellers, J Chem. Eng. Jpn., **29**, 51-58, (1996).
4. Chhabra, R.P and Richardson, J.F., Non-Newtonian Flow and Applied Rheology, 2nd edition, Oxford, Butterworth-Heinemann (2008).
5. Cooke M., Rodgers T.L., Kowalski A. J., Power Consumption Characteristics of an In-Line Silverson High Shear Mixer, AIChE, **58**, 1683-1692, (2012).
6. Darby R., Viscoelastic fluids-An introduction to their properties and behavior, New York, Markel Dekker Inc., (1976)
7. Delplace F., Leuliet J.C, “Generalized Reynolds number for the flow of Power-law fluids in cylindrical ducts of arbitrary cross-section”, Chem. Eng. J. **56**, 33-37 (1995)
8. Doran P., Bioprocess Engineering Principles 2nd edition, U.K., Academic Press, (2013)
9. Ferguson J., Kemblowski Z., Applied fluid rheology, London, Elsevier Applied Science, (1991)
10. Han C.D., J., Measurement of the rheological properties of polymer melts with slit rheometer. I. Homopolymer systems, Appl. Polym. Sci, **15**, 2567-2577, (1971)
11. Hanks R.W and Larsen K.M., The flow of power-law Newtonian fluids in concentric annuli, Ind. Eng. Chem. Fundamen., **18,** 33-35, (1979).
12. Hartnett JP, Kostic M, Adv Heat transfer, **19**, 247-356, (1989)
13. Kozicki W., Chou C.H, Tiu C, Non-Newtonian flow in ducts of arbitrary cross-sectional shape, Chem. Eng. Sci, **21**, pp 665-679; (1966)
14. Kresta S.M, Etchells A.W, Dickey S. D, Obeng-Atiemo V.A., Advances in industrial mixing, 1st Edition, Willey, U.S. (2016).
   Macosko C.W., Rheology: Principles, measurements, and applications, Wiley-VCH, New York (1994)

15. Malkin Y.A., Isayev A. I., Rheology- Concept methods and applications 3rd edition, ChemTec, Toronto (2017).
16. Metzner A.B, Reed J.C., Flow of non-Newtonian Fluids- Correlations of the laminar, transition and turbulent flow regions, AlChe J. 1, 434-440 (1955).
17. Metzner A. B., Otto R.E., Agitation of non-Newtonian fluids, AIChe J. **3**, 3-11 (1957).
18. Morrinson A. F., Understanding rheology, Oxford University Press, New York (2001)
19. Netusil J., F. Rieger, Power consumption of screw and helical ribbon agitators in highly viscous pseudoplastic fluids, Chem. Eng. J., **52**, 9-12, (1992)
20. Osswald T., Rudolph N., Polymer rheology, Munich, Hanser Publication, (2015)
21. Paul E.L., Atiemo-Obeng V.A., Kresta S.M., Handbook of industrial mixing: Science and application, 1st edition, John Wiley & Sons, Inc, Canada, (2004).
22. Rieger F., Novak V. Power consumption of agitators in highly viscous non-Newtonian fluids, Trans. Inst. Chem. Eng. 51, 105-111 (1973).
23. Rieger F., Novak V., Power consumption scale-up in agitating non-Newtonian fluids, Chem. Eng. Sci. **29**, 2229-2234, (1974).
24. Skočilas J, R. Žitny R, Štancl R., Flow of bovine collagen in rectangular slit, AIP conference proceedings, **1843, (**2017)
25. Skočilas J, R. Žitny R, Štancl R, M. Dostal, J. Rheological Properties of Collagen Matter Predicted Using an Extrusion Rheometer, Texture stud. 47, 514-522 (2016).
26. Son Y., Determination of shear viscosity and shear rate from pressure drop and flow rate relationship in a rectangular channel, Polymer, **48**, 632-637, (2006).
27. Šesták, J, Rieger F., Prenos Hybnosti, Tepla a Hmoty, Vydavatelstvi CVUT Praha (2005).
28. Utomo A. T (2009), Flow patterns and energy dissipation rates in batch rotor-stator mixers (Doctoral dissertation), The School of Engineering of The University of Birmingham, U.K.
29. Vial C., Stiriba Y., Trad Z., CFD Simulation of Flow and Mixing in In-line Rotor-Stator Mixers with Complex Fluids, Can J. Chem Eng. **93**, 391-403, (2015).
30. Vicente D., J, Rheology, InTech., Crotia, (2012)
31. Zhang C. Gu J., Qin H., Xu Q. Li W., Jia X., Zhang J., CFD analysis of flow pattern and power consumption for viscous fluids in in-line highs hear mixers, Chem. Eng. Res. Des., **117**, 190-214, (2017).

List of Author's Publications

1. Ayas M. Skocilas J. and Jirout T., A practical method for predicting the friction factor of power-law fluids in a rectangular duct. Chem. Eng. Commun., **206**, 1310-1316, (2019).
2. Ayas M., Skocilas J., and Jirout T., Friction factor of shear thinning fluids in non-circular ducts – a simplified approach for rapid engineering calculation, Chem. Eng. Commun. doi.org/10.1080/00986445.2020.1770232, (2020). (Published online-article in press)
3. Ayas M., Skocilas J. and Jirout T., Analysis of Power Input of an In-Line Rotor-Stator Mixer for Viscoplastic Fluids, Processes, **8**, 1-15, (2020).
4. Ayas M., Skocilas J. and Jirout T., A method for the determination of shear viscosity of power-law fluids in a rectangular duct and concentric annulus, Asia-Pac. J. Chem. Eng. (Under review).